Experimental Investigation of a Simulated Compressor Airfoil Trailing-Edge Flowfield

Robert W. Paterson*
United Technologies Research Center, East Hartford, Connecticut
and
Harris D. Weingold†
Pratt & Whitney Aircraft Group, East Hartford, Connecticut

This study was motivated by the need for improved understanding of blunt trailing-edge compressor airfoil flowfields. The objective was to provide data that could be used to assist the development of computational procedures for predicting such flows. A large-scale, low subsonic Mach number, wind tunnel simulation of a compressor airfoil trailing-edge flowfield was conducted using a flat-plate test model and laser Doppler velocimetry for flowfield definition. Of potential importance in the numerical modeling of the flow was the finding that outer flow velocity profiles in the near wake were nearly identical, with viscous interaction effects confined to a region near the wake centerline having a thickness and length comparable to that of the trailing-edge thickness. Qualitative agreement with circular cylinder near-wake data and an observed lack of dependence of results on a change in plate boundary-layer thickness suggest that the flow is not strongly dependent on boundary-layer thickness at separation. Periodic vortex shedding was encountered and shown to affect base pressure significantly. The associated strong transverse velocity fluctuations would be expected to be the dominant mechanism for mixing out the velocity defect in the initial wake region.

Introduction

COMPRESSOR airfoils are designed, for structural and durability reasons, with thick rounded trailing edges that cause trailing-edge boundary-layer separation and attendant flow recirculation and unsteadiness. The principal analysis used in the design of high-performance supercritical compressor airfoils is an inviscid transonic cascade calculation coupled to a boundary-layer calculation. The resultant designs can be influenced significantly by the modeling of the blunt trailing edge in the inviscid analysis. Imposition of an inviscid Kutta condition produces calculated pressure spikes near the trailing edge, which in turn influence the calculated boundary layer further upstream. Data suggest that the actual viscous flowfields present in such geometries moderate the magnitude of these spikes. Therefore, improved prediction of the turbulent, separated blunt trailing-edge flowfield is important to the design process.

A recent review of the application of viscous-inviscid interacting flow theory to the trailing-edge problem is given by Werle.[1] For this or other numerical approaches, experimental data are required to assess the accuracy and assist the development of trailing-edge flow computational procedures. Presently, however, there is a general lack of experimental data on thick, rounded trailing-edge flowfields. [Circular cylinders, thin plates (or airfoils) with sharp trailing edges, and thick trailing-edge configurations with salient edges (and hence fixed separation points) have received the most attention. Even for this wide range of geometries, the number of detailed near-wake investigations with turbulent boundary-layer separation is surprisingly limited.] A large-scale cascade investigation by Hobbs et al.[2] delineated certain features of such flows but also indicated the need for experimentation at larger scale than that achievable in cascade (trailing-edge thicknesses on the order of several millimeters). The present study, described in more detail elsewhere,[3,4] was undertaken to provide detailed code assessment data at large scale.

Approach

Model geometry and flow conditions were selected that would provide simple, yet relevant, test cases to which predictions of a computational procedure could be compared. The scale of the experiment (1-in. thick circular arc trailing edge) was determined by the need to acquire a detailed definition of the velocity and pressure fields in the vicinity of the trailing edge. A flat-plate model was selected since compressor airfoil curvature is small in the trailing-edge region. Relative to flow conditions, the approach was to conduct the experiment at low subsonic Mach number in a two-dimensional flow environment. Modeling of compressibility effects was not considered to be of first-order importance in determining the suitability of a code to treat blunt trailing-edge flows.

The remaining flow condition of interest was the nature of the boundary layers incident upon the trailing-edge region. For full-scale engine compressor blades, boundary layers near the trailing edge are turbulent and thicknesses and shape factors vary over an appreciable range. The approach taken here was to conduct the experiment with two different sets of initial boundary-layer conditions and with the absolute value of boundary-layer-thickness to trailing-edge thickness ratio in the range expected for typical supercritical airfoil designs. One set of initial conditions consisted of equal thickness turbulent boundary layers on the two surfaces of the plate. This symmetrical boundary-layer configuration was intended to provide the simplest test case for code assessment purposes. It was considered desirable that the symmetrical configuration boundary layers have characteristics close to those obtained in a zero-pressure gradient environment. This would provide near-equilibrium boundary-layer "initial conditions" that

Presented as Paper 84-0101 at the AIAA 22nd Aerospace Sciences Meeting, Reno, Nev., Jan. 9-12, 1984; received Jan. 12, 1984; revision received June 20, 1984.

*Manager, Aeroacoustics and Experimental Gas Dynamics. Associate Fellow AIAA.

†Senior Research Engineer. Associate Fellow AIAA.

could be generated by boundary-layer codes. The second set of initial conditions consisted of unequal thickness turbulent boundary layers on the two surfaces. In this asymmetrical configuration test case, it was desired to achieve a substantial difference in relative thickness (on the order of 2). Comparison of symmetrical and asymmetrical configuration results was intended to provide insight into the importance of variations in initial viscous conditions in the absence of trailing-edge loading effects (pressure-to-suction surface differential pressure).

Experimental Arrangement

Test-plate length was determined by the need to generate thick boundary layers (relative to trailing-edge thickness) characteristic of compressor airfoils. Typical boundary-layer characteristics for supercritical airfoils are given by the Build I cascade data reported by Hobbs et al.[2] At a position 0.032 chord upstream of the trailing edge, ratios of pressure and suction surface momentum thickness to trailing-edge diameter were 0.09 and 0.26, respectively. To achieve relative thicknesses in this range, a natural boundary-layer development length in excess of 3 m was required.

The resultant test model, shown in Fig. 1, consisted of a 3.65-m-long (axial direction), 1.07-m-wide (spanwise direction), 2.54-cm-thick flat plate equipped with a 3:1 elliptical leading-edge fairing. The large ratio of plate width to thickness (42) was chosen to yield two-dimensional flow conditions in the midspan region over the axial extent (approximately 15 plate thicknesses) of the trailing-edge interaction region. Whereas the overall plate aspect ratio was 0.34, the aspect ratio relevant to two-dimensional flow (lack of significant stream convergence due to sidewall boundary-layer growth) in the trailing-edge interaction region was much larger (42/15). The leading-edge region of the plate was flared outward in the spanwise direction to fit the contour of the wind tunnel inlet contraction. The study was conducted in the United Technologies Research Center Open-Jet (Acoustic) Wind Tunnel,[5] an open-circuit, low turbulence level (0.2%), subsonic wind tunnel. The open-jet test section is surrounded by a $4.5 \times 5 \times 6$ m sealed chamber. A schematic of the model installation in the tunnel is shown in Fig. 2. The aft end of the plate extended 0.48 m into the open-jet test section of the tunnel. In addition to the use of a large span-to-thickness ratio to minimize end effects, 90-deg circular arc sideplate extensions, shown in Fig. 2, were installed at the nozzle exit to reduce open-jet shear-layer penetration into the test section near the ends of the plate. The upper and lower quadrants of the test section in the region of the sideplates were left open. To produce the asymmetrical boundary-layer test condition, the ramp fairing shown in Fig. 2 was employed. For the symmetrical case, no ramp was provided and the turbulent trips were installed at the plate leading edge. For the asymmetrical case, the lower surface trip was moved to a plate position aft of the ramp.

Test Program Definition

Based upon code assessment requirements and experimental considerations, the axial and transverse mean and fluctuating velocity components, total pressure, reference total temperature, reference static pressure, wake centerline static pressure, and surface static pressure were selected as the variables to be measured directly. In regions where total pressure measurements were reliable, total pressure and velocity data could be used to calculate flowfield static pressure within certain error bounds. To meet the code assessment objective, a "benchmark" experiment must provide data at a location to start the computation and at relevant locations to determine prediction accuracy. A plane normal to the plate located upstream of the trailing edge (termed the initial measurement plane) was selected to provide starting conditions. Hot-wire anemometry was used to define velocity profiles in this plane. To assess velocity and displacement surface predictions, laser Doppler velocimetry (LDV) was employed to measure the axial and transverse velocity components in approximately ten planes located between the start of the trailing-edge circle and six plate thicknesses downstream of the trailing edge.

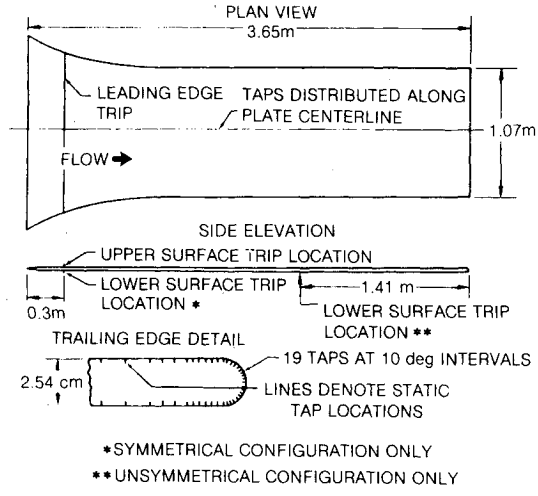

Fig. 1 Flat plate model geometry.

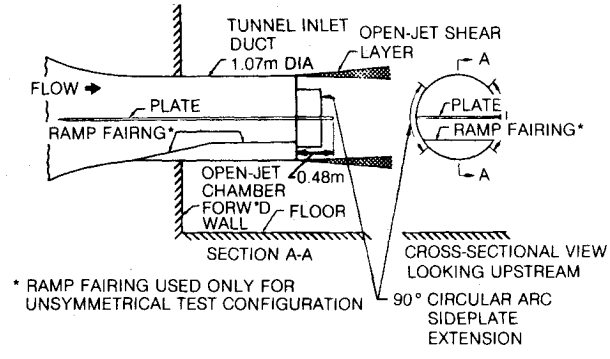

Fig. 2 Open-jet wind tunnel installation.

Table 1 Asymmetrical configuration initial plane parameters

	Upper surface	Lower surface
δ^*/t	0.221	0.133
θ/t	0.173	0.097
δ^*/θ	1.28	1.38

Objectives were identified at the outset of the experiment regarding symmetry of measured quantities relative to the plate centerline for the symmetric boundary-layer configuration, and spanwise uniformity of initial plane velocity profiles for both configurations. Agreement of upper and lower surface boundary-layer integral properties within 5%, at the initial measurement plane, was established as an objective for symmetrical configuration profiles. The same tolerance was identified for the spanwise uniformity of profiles in the initial plane. Agreement of individual velocity components, above and below centerline, for the symmetrical configuration, was expected to be within 3% of the reference velocity, based upon LDV measurement uncertainty estimates.

The experiment was conducted at a constant Reynolds number of 8.1×10^6 (based on plate length). Since tunnel stagnation temperature varied with atmospheric conditions, the tunnel Mach number was varied from 0.09 to 0.1 to main-

	UPPER SURFACE		LOWER SURFACE	
	MEAS	PRED	MEAS	PRED
δ^*/t	0.1894	0.1821	0.1768	0.1786
θ/t	0.1439	0.1379	0.1349	0.1355
δ^*/θ	1.316	1.320	1.311	1.319

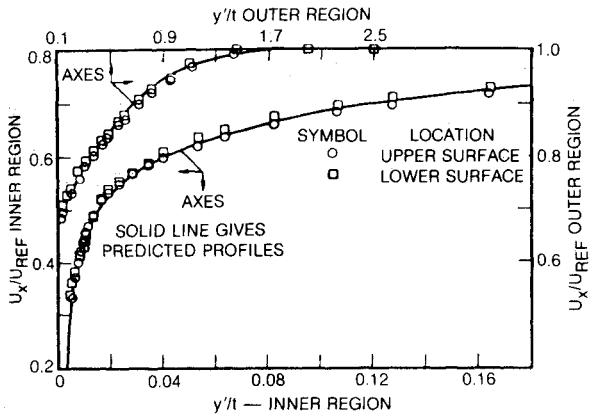

Fig. 3a Symmetrical configuration initial plane velocity profiles (plate centerline, $x/t = -10.6$).

	UPPER SURFACE		LOWER SURFACE	
	MEAS	PRED	MEAS	PRED
C_f	0.00278	0.00269	0.00287	0.00272
$C_f Re_\theta$	22.6	21.9	21.9	21.6

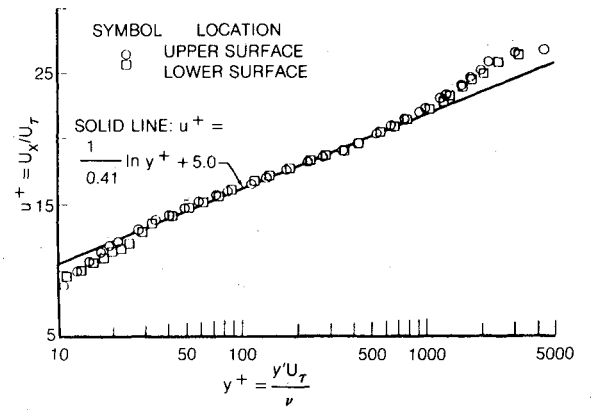

Fig. 3b Symmetrical configuration initial plane near-wall velocity profiles (plate centerline, $x/t = -10.6$).

tain a constant Reynolds number. Measured velocities were normalized by freestream velocity, U_{REF} (open-jet test section velocity). The difference between a measured static pressure p and freestream static pressure p_{REF} was normalized by tunnel dynamic pressure $\rho U_{REF}^2/2$ to yield the pressure coefficient C_p. These normalized quantities were shown to be invariant with respect to tunnel speed changes, as would be anticipated.

Experimental Results

Initial Measurement Plane Conditions

Plate boundary-layer conditions approaching the trailing-edge interaction region were defined in an initial measurement plane located 10.6 plate thicknesses upstream of the trailing edge. Average boundary-layer thicknesses (normalized by plate thickness) and related parameters obtained at midspan in this plane for the symmetric configuration are tabulated as: 99.5% thickness, $\delta/t = 1.47$; displacement thickness, $\delta^*/t = 0.183$; momentum thickness, $\theta/t = 0.139$; shape factor, $H = 1.31$; and momentum Reynolds number $Re_\theta = 7860$. These

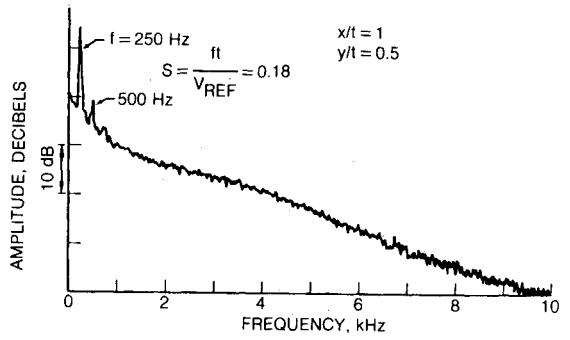

Fig. 4 Wake hot-wire spectrum.

values represent the average obtained above and below the plate. The boundary-layer thickness was approximately 1.5 plate thicknesses with the momentum thickness about one-seventh of the plate thickness. The measured shape factor of 1.31 was reasonably close to the value of 1.33 quoted by Coles[6] for a constant-pressure turbulent boundary layer at the measured momentum thickness Reynolds number of 7860. This is an indication that a near-equilibrium, zero-pressure gradient boundary-layer initial condition was achieved.

Initial measurement plane velocity profiles obtained at midspan showed that 1) a nearly symmetrical (upper surface vs lower surface) boundary-layer configuration was obtained, and 2) good agreement between measured profiles and predictions of the UTRC ABLE[7] code was achieved. Figure 3a provides these profile data in the form of axial velocity U_x normalized by freestream reference velocity U_{REF} as a function of distance normal to the plate y'. Circular symbols correspond to measurements above the plate and square symbols correspond to measurements below the plate.

In terms of upper-lower surface boundary-layer symmetry, individual data points tend to agree within 1%. Differences between upper and lower surface displacement and momentum thickness were close to the 5% tolerance identified at the outset of the experiment. Figure 3a also compares data to the predictions of the ABLE boundary-layer code. In this figure, the inner region axes are to the left and bottom while the outer region axis scales are at the top and to the right. Shown differences between upper and lower surface predictions were due to the slightly different plate static distributions input to the code (and shown subsequently). The favorable comparison of predicted and measured results indicates that a boundary-layer code can be used to provide initial conditions for computational procedures used to predict the plate trailing-edge interaction. In addition to these code comparisons, profile data were found to be in good agreement with law of the wall,[6] as shown in Fig. 3b.

Initial plane boundary-layer integral properties for the asymmetrical test configuration are given in Table 1. The ratio of upper-to-lower surface momentum thickness of 1.8 was reasonably close to the desired value of approximately 2.

Vortex Shedding

Vortex shedding from the plate trailing edge occurred with both symmetrical and asymmetrical boundary-layer test configurations. A clear indication of this was the presence of an audible tone in the test chamber. Hot-wire measurements, obtained in the wake of the plate, confirmed a strong discrete frequency signal at approximately 250 Hz (depending on tunnel speed), which, when normalized by plate thickness and freestream velocity, resulted in a Strouhal frequency of 0.18. A typical wake hot-wire spectrum, showing the magnitude of this discrete frequency signal relative to the broadband (random) wake turbulent signal, is shown in Fig. 4. This figure displays an off-centerline spectrum which is dominated by the 250-Hz frequency associated with the fundamental period of

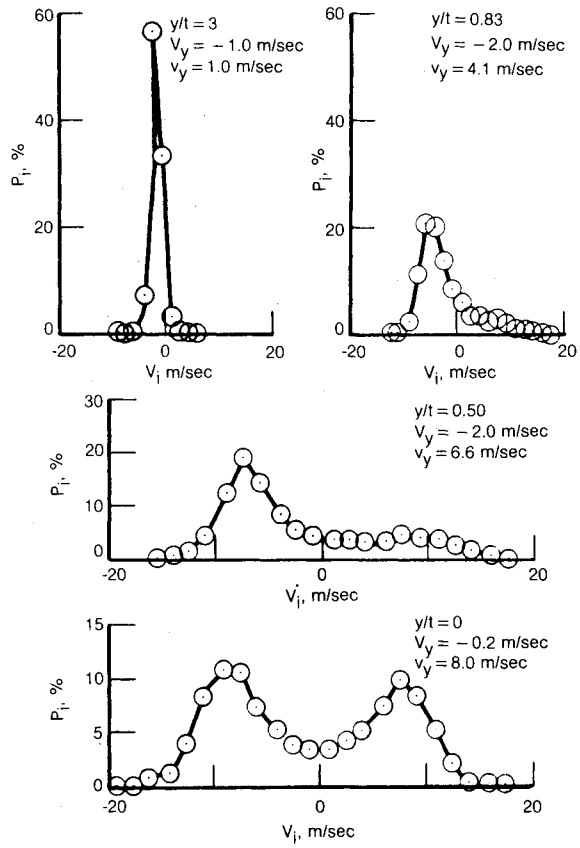

Fig. 5 LDV probability distributions for transverse velocity component in the wake ($x/t = 3$).

the shedding cycle (the period of shedding from one surface). On the plate centerline, the dominant frequency was a factor of 2 higher since the hot wire responded to shedding from both upper and lower plate surfaces.

Vortex shedding had a strong influence on the nature of the LDV probability density distributions obtained in the wake. Shown in Fig. 5 is a sequence of distributions for the vertical velocity component starting three plate thicknesses above the plate ($y/t = 3$) and proceeding to the wake centerline at a fixed axial position of $x/t = 3$. Plotted is the percentage of LDV seed particles which had an instantaneous velocity of V_i during the period of time required to acquire 3000 validated seed particle counts. Listed in each part of the figure are the vertical mean velocity component V_y and vertical rms velocity fluctuation component v_y, which were calculated from the shown probability distributions. At a position above the plate and removed from the centerline ($y/t = 3$), the probability distribution was narrow and the calculated rms fluctuation low (1 m/s) relative to the local axial velocity of 33 m/s. As the plate centerline was approached, the distribution broadened and the rms level increased. On centerline, $y/t = 0$, the probability distribution had acquired a nearly symmetrical double-peaked shape resulting in a calculated near-zero vertical mean velocity component. The broadened distribution caused the calculated fluctuating component to increase by a factor of 8 relative to the $y/t = 3$ value. While the calculated mean velocity was zero, Fig. 5 indicates that the flow resided at ±8 m/s a much higher percentage of the time. It remains to be seen whether a time-independent code can account for the axial momentum transfer associated with this transverse mixing by appropriate adjustment of the turbulence model.

At positions below the plate the distributions were similar[3] in character to those above the plate, although reversed in sign, as would be expected if this were due to a symmetrical upper and lower surface shedding process. By an independent test, it was established that the behavior described above was

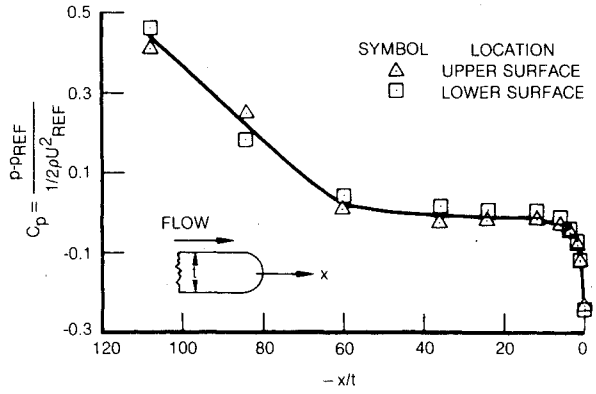

Fig. 6 Symmetrical configuration overall surface static pressure distributions.

due to the presence of vortex shedding. A splitter plate was installed on the wake centerline, extending from the test-plate trailing edge to eight plate thicknesses downstream. It is known that introduction of a solid boundary of this length between shear layers emanating from a bluff body suppresses vortex shedding. When measurements were obtained with this plate installed, the double-humped character of the vertical component LDV probability distributions was eliminated.

In a recent thesis by Haji-Haidari,[8] bubble-wire flow-visualization results for a thick, circular geometry trailing-edge flowfield are given as well as comparison of hot-wire profiles with a tapered trailing-edge geometry having no vortex shedding. A conclusion of the study is that wake mixing is strongly enhanced by the shedding process.

Static Pressure Distributions

For the symmetrical boundary-layer configuration test condition, the test plate was aligned within the tunnel inlet nozzle to produce nearly equal static pressure distributions on the upper and lower plate surfaces, as shown in Fig. 6. Following a region of favorable pressure gradient associated with the projection of the plate leading edge into the wind tunnel contraction, a region of near-zero pressure gradient existed from about $x/t = -60$ to -10. From the rapid decrease in static pressure between $x/t = -10$ and 0, it is apparent that the trailing edge influences the approaching flowfield over a significant distance upstream of the actual edge. A more detailed definition of the trailing-edge pressure distribution as well as wake centerline pressure measurements for the symmetrical test configuration are shown in Fig. 7. Wake centerline static pressure measurements were obtained by positioning the static pressure ports of a small (1.6 mm) cylindrical tube at various axial positions along the centerline. To avoid leading-edge flow disturbances that would exist with conventional static pressure probes, the tube extended upstream into the plate. As the tube was withdrawn from inside the plate, a ring of four static ports drilled at one axial position of the tube traversed the wake. The tube was extended downstream of the ports to eliminate interference from end effects. This procedure is subject to some uncertainty since the cylindrical tube is subjected to a time-dependent crossflow associated with vortex shedding transverse velocity fluctuations. The multiport averaging is believed to have minimized errors due to this fluctuating field.

Based on static pressure measurements at 10-deg increments on the trailing-edge circle, a minimum pressure coefficient of −0.25 was observed to occur at an azimuth angle of 80 deg relative to the trailing edge. Surface flow-visualization results, discussed subsequently, indicated that separation occurred at approximately 76 deg. Within the 10-deg resolution in static pressure measurements, the onset of an adverse pressure gradient and location of separation were therefore in close agreement. The wake centerline measurements, denoted by the circles in Fig. 7, show that the near-wake static pressure

decreased abruptly from its trailing-edge value, reached a minimum at $x/t=0.375$, and then increased monotonically, approaching freestream static pressure at $x/t=3.5$. Based on LDV measurements discussed subsequently, the length of the recirculation region downstream of the plate was approximately $0.8t$. The wake pressure minimum, therefore, occurred near the midpoint of this region.

In 1954, Roshko[9] demonstrated that a similarly strong wake centerline pressure minimum existed behind circular cylinders undergoing vortex shedding and this minimum was associated with the vortex formation process. By extending a splitter plate downstream of the cylinder on the wake centerline, Roshko suppressed vortex shedding and observed a significant reduction in the magnitude of the pressure minimum. To determine whether vortex formation was the cause of the abrupt decrease in static pressure just downstream of the trailing edge in the present study, wake centerline static pressure measurements were acquired with the previously described trailing-edge splitter plate installed. Static pressure taps in the plate were used to obtain these data. As shown in Fig. 8, the effect of the splitter plate was to alter the trailing edge and wake static pressure distribution significantly. In addition to reducing the magnitude of the near-wake static pressure depression, static pressure increased above the freestream value further downstream. Vortex shedding, therefore, appears to be important in determining the nature of the plate trailing edge and wake static pressure distribution. This is consistent with the findings of Roshko who concluded that, for both flat plates normal to the flow and for cylinders, "The main mechanism for the base pressure is to be found not in the diffusion of momentum across the shear layers but in the dynamics of the vortices." This similarity between cylinders and the present case occurred even though the ratio of boundary-layer thickness at separation to trailing-edge circle (or cylinder) diameter was significantly larger here.

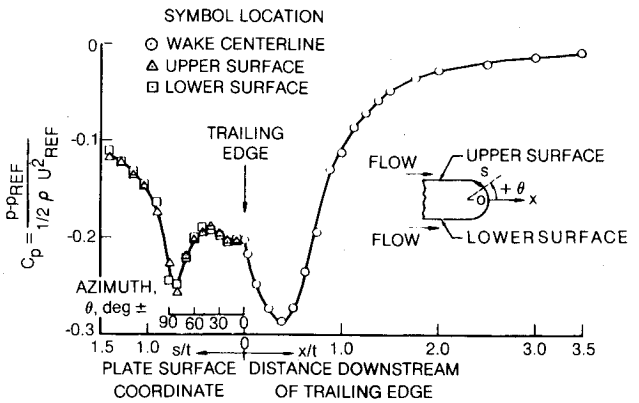

Fig. 7 Symmetrical configuration trailing-edge and wake centerline static pressure distributions.

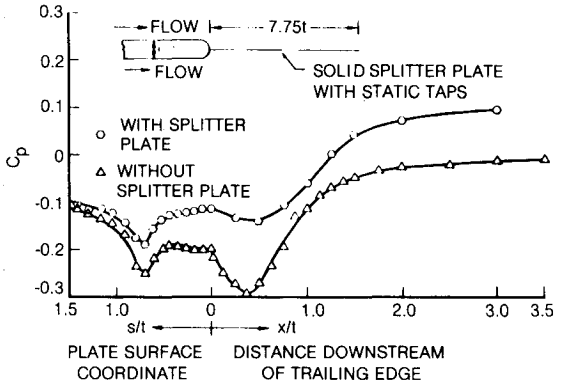

Fig. 8 Effect of wake splitter plate on static pressure distribution.

For the asymmetric test configuration, the plate static pressure distributions were significantly different on the upper and lower surfaces (as a result of the ramp fairing) except in the trailing-edge region, $-6<x/t\leq 0$, where they were not only identical but indistinguishable from those for the symmetrical case.[3]

Flow Visualization

Surface flow visualization of the plate trailing-edge region was performed to define separation lines. For symmetrical and asymmetrical configurations, separation lines on the upper and lower surfaces were found to be straight, over a spanwise extent greater than six plate thicknesses, with a maximum deviation of 1 deg of arc from a mean separation location of approximately 14 deg (as measured from the tangency point of the plate and trailing-edge circle). Flow visualization photographs are given elsewhere.[3] The tests confirmed surface static pressure results which had suggested that separation locations were similar for both upper and lower surfaces and both boundary-layer configurations. The straight separation lines were consistent with the expectation of two-dimensional flow conditions.

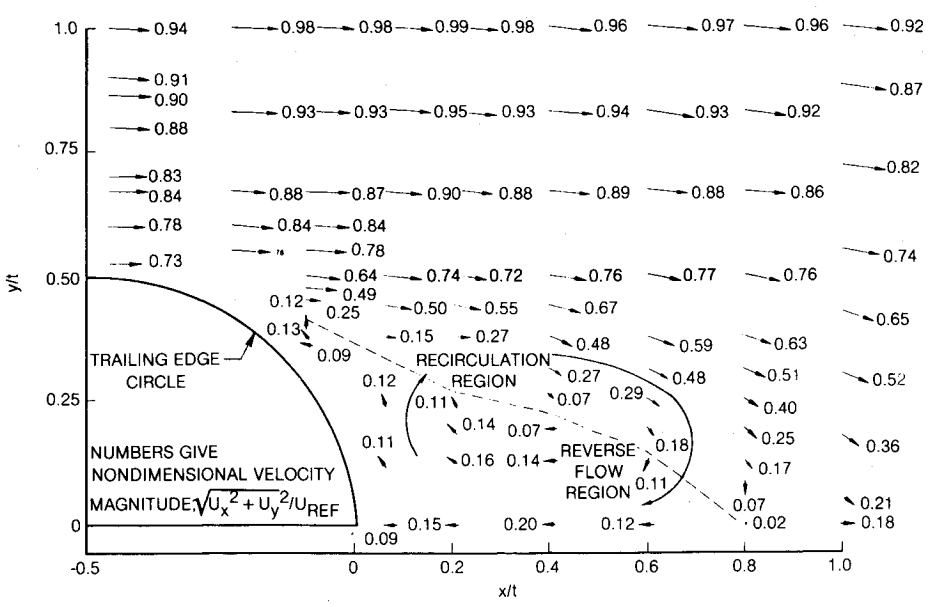

Fig. 9 Symmetrical configuration near-wake velocity field.

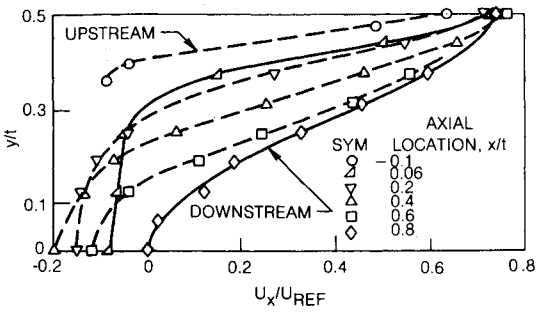

Fig. 10a Symmetrical configuration inner region axial velocity distributions.

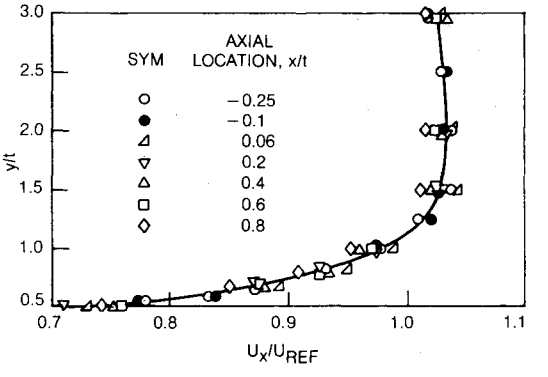

Fig. 10b Outer region axial velocity distributions.

Symmetrical Configuration Mean Velocity Field

LDV was employed to define the axial and transverse (vertical) mean velocity components from the start of the trailing-edge circle ($x/t=-0.5$) to 6.5 plate thicknesses downstream of the trailing edge. The general character of the near-wake velocity field is displayed in Fig. 9. Only data for $y>0$ are shown since $y<0$ data agreed within the estimated 3% velocity measurement uncertainty bound. In the figure, vectors indicate local flow direction and associated numbers provide velocity magnitude relative to the open-jet test-section velocity, U_{REF}. The region containing vectors having an upstream axial component is shown bounded by a dashed line. Interpolation between neighboring data points was used to define this line.

The axial extent of the reversed-flow region on the plate centerline is seen to be $0.8t$ with a maximum reversed-flow velocity of 20% of freestream achieved at the midpoint ($x/t=0.4$) of the region. In a study of a cylinder near wake, Owen[10] found that mean wake closure occurred 0.8 diameter behind the cylinder trailing edge, in agreement with the 0.8 plate thickness value obtained here. This occurred despite the fact that the cylinder boundary layers at separation were thin compared to those of the present study.

Figure 10a provides profiles of the mean axial velocity component at axial locations close to the trailing edge ($x/t<0.8$) and for the "inner" region of the wake (where "inner" is defined as that portion of the wake between the wake centerline and the plate surface extended, $y=0.5t$). In this region, profiles are observed to vary significantly although there is a trend toward coalescence of profiles at $y/t=0.5$. This is explored further in Fig. 10b where profiles for the "outer" region ($y/t>0.5$) are shown at an expanded velocity scale relative to Fig. 10a. Deviations from the curve faired through the data are observed to be very small (typically within 1 or 2%) for axial positions ranging from upstream of the trailing edge ($x/t=-0.25$) to the wake closure point ($x/t=0.8$). As noted by Werle,[1] the outer flow, over the axial extent of the recirculation zone, appears to act as a basically

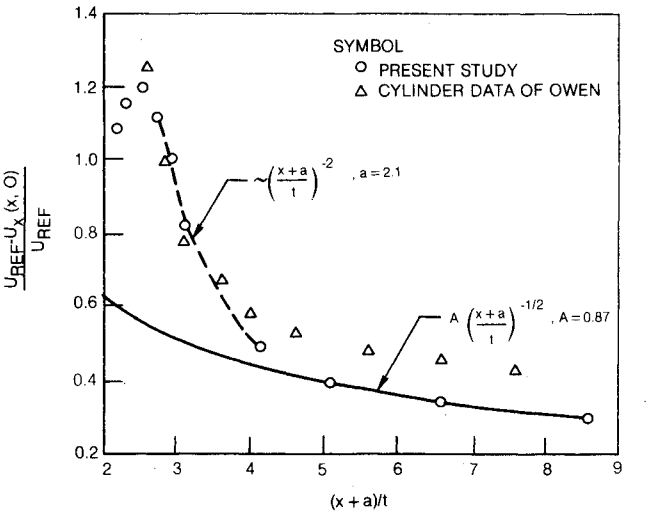

Fig. 11 Comparison of wake centerline axial velocity distribution with cylinder wake results of Ref. 10.

inviscid rotational flow with viscous-induced velocity profile alterations confined to the inner region. This observation provides support for the numerical modeling of this flow by viscous-inviscid interaction theory.

The wake centerline axial velocity behavior is shown in Fig. 11, where normalized wake defect has been plotted as a function of normalized downstream distance $(x+a)/t$, a being an empirically derived parameter. For cylinders, the far-wake axial velocity defect is predicted, and found experimentally to follow, a decay law of the form[11]:

$$\frac{U_{REF}-U_x(x,0)}{U_{REF}}=A\left(\frac{x+a}{d}\right)^{-1/2}$$

where A is proportional to the drag coefficient of the cylinder and a the distance between the cylinder axis and the upstream origin of similarity (virtual origin). The figure shows that a similar decay relationship can be fitted to the present data at distances greater than approximately two plate thicknesses downstream of the trailing edge. At positions closer to the trailing edge, the decay rate is much more rapid, having a negative second power dependence. The cylinder near-wake measurements of Owen[10] follow a similar pattern, as indicated by the triangular symbols in Fig. 11.

Further general agreement between plate and cylinder wake results is given by the axial velocity correlation shown in Fig. 12. Plotted is the ratio of the off-axis wake defect to the measured wake centerline defect as a function of the parameter ξ used to correlate cylinder far-wake results.[11] The constant $a=2.1$, derived from Fig. 11, has been retained and the constant of 0.45, appearing in the exponent, has been chosen to fit the off-axis velocity profile data. The Gaussian form of the wake defect correlation, shown in the figure, results from both a far-wake and a constant eddy-viscosity assumption.[11] Using a constant of 0.26, instead of the 0.45 value employed here, the Gaussian relationship has been shown to be in close agreement with Townsend's cylinder far-wake data. Thus, while constants differ, the off-axis axial velocity correlation provides a second example (in addition to the previously discussed wake centerline correlation) in which use of a far-wake assumption provides results relevant to the plate near-wake case.

The displacement surface location in the plate near-wake region for the symmetrical configuration is shown in Fig. 13. Plotted is the sum of displacement thickness calculated from the axial velocity profiles and the height of the trailing-edge surface relative to the centerline h ($h=0$ for $x\geq 0$). The loca-

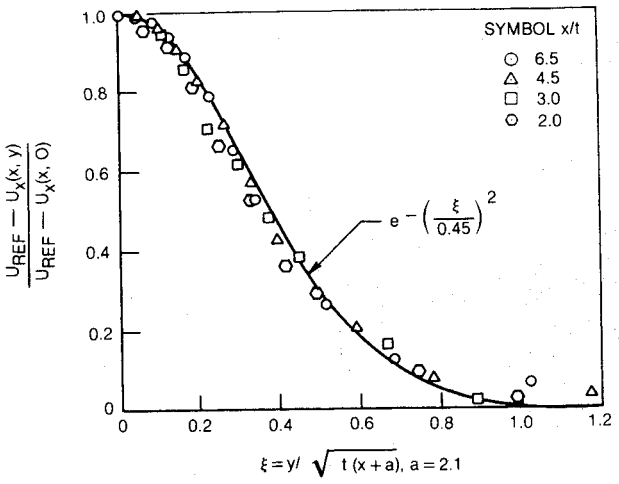

Fig. 12 Wake axial velocity component correlation.

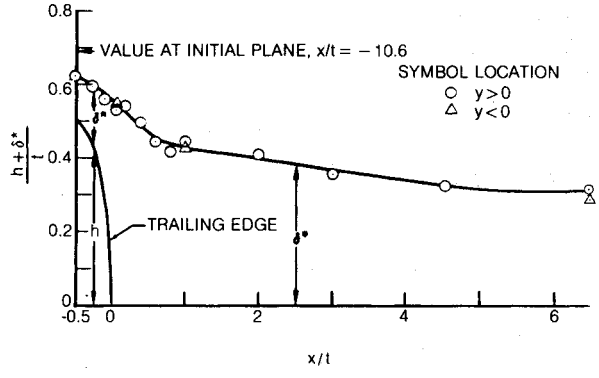

Fig. 13 Displacement surface location.

tion of the displacement surface at the initial measurement plane ($x/t = -10.6$) is indicated by an arrow. Between this plane and the start of the trailing-edge circle ($x/t = -0.5$), the displacement surface decreases in height. A rapid decrease occurs in the immediate vicinity of the trailing edge ($-0.5 \le x/t \le 1.0$). In the far wake, theory[11] predicts a constant value for the displacement thickness. A gradual approach to a constant value is indicated in the figure.

The displacement surface results, as well as previously discussed wake centerline and off-centerline axial velocity correlations, indicate that the flowfield begins to assume far-wake characteristics at a distance approximately two to three plate thicknesses downstream of the trailing edge.

Transverse mean velocity component data are provided elsewhere.[3] The maximum measured outwardly directed component was 12% of freestream velocity, obtained at $x/t = -0.1$; the maximum component directed toward the wake centerline was 22% of freestream, measured at the end of the recirculation region, $x/t = 0.8$.

Asymmetrical Configuration

Axial velocity profiles, the displacement surface location, and the wake centerline velocity distribution were nearly the same for this configuration as for the symmetrical. Some differences were noted in transverse velocity profiles and, to a lesser extent, in the displacement surface location.[3] Overall, the velocity data confirmed the similarity of the two configurations inferred from pressure measurements and flow visualization. These results apply to a change in relative boundary-layer thickness at a nearly constant shape factor (δ^*/θ of 1.28 on the upper surface and 1.38 lower) in the absence of trailing-edge differential loading. In this situation the lack of a relative shift in upper and lower surface separation locations is understandable. With similar separation locations and a large-scale vortex dominated near-wake mixing process, the lack of noticeable velocity profile asymmetry downstream of the trailing edge also appears reasonable.

Total Pressure Measurements

A conclusion of the referenced detailed report of this investigation[3] is that total pressure measurements close to the trailing edge cannot be used in conjunction with LDV velocity data to calculate the wake static pressure field in a sufficiently accurate manner to be meaningful. The primary source of the error is believed to be the unknown effect of the strong unsteady velocity field on the measurement of total pressure. Total pressure data, while not reported here or in the referenced publications,[3,4] are available from the authors.

Conclusions

1) Trailing-edge surface pressures and wake static pressures were strongly influenced by the presence of vortex shedding from the plate trailing edge. Installation of a splitter plate at the trailing edge suppressed vortex shedding and reduced the base region static pressure depression in a manner similar to that observed in experiments with circular cylinders.

2) The ratio of boundary-layer thicknesses on the two surfaces of the plate in the trailing-edge region does not appear to be a critical parameter in determining the character of the near-wake flowfield. A change in thickness ratio by a factor of 1.8 (at nearly constant shape factor and in the absence of trailing-edge loading) had a negligible influence on the location of separation points, surface pressures, and axial velocity distributions. Inclusion of trailing-edge loading in subsequent simulation experimentation would be expected to contibute to improved understanding of trailing-edge flowfields.

3) Viscous-induced velocity profile alterations were confined to a region near wake centerline having a thickness comparable to the trailing edge. Over the axial extent of the recirculation region, the outer flow acted as a basically inviscid rotational flow.

4) Vortex shedding would be expected to be a more important mechanism for lateral transport of axial momentum in the near-wake region than turbulence.

5) The trailing-edge interaction region, as indicated by static pressure distributions, extended from about ten plate thicknesses upstream of the trailing edge to three plate thicknesses downstream of the edge. At distances greater than two to three plate thicknesses downstream of the trailing edge, axial velocity data could be correlated using functional relationships applicable to the far wake.

6) The axial extent of the reversed-flow region downstream of the trailing edge was approximately eight-tenths of the plate thickness. This was similar to results reported for cylinders when plate thickness and cylinder diameter were taken as the relevant length scales for comparing plate and cylinder results.

7) Qualitative agreement of other plate and circular cylinder near-wake velocity data suggests that the absolute value of boundary-layer thickness to plate trailing-edge thickness is not a critical parameter in determining the near-wake flowfield.

Acknowledgments

The study reported herein was performed for Naval Air Systems Command under Contract N00019-80-C-0633. The authors wish to acknowledge helpful discussions with Dr. M. J. Werle (UTRC), Prof. E. M. Greitzer (M.I.T.) and Messrs. J. K. Schweitzer, D. E. Hobbs, and J. F. Dannenhoffer III of Pratt & Whitney Aircraft.

References

[1]Werle, M. J., "Compressor and Turbine Blade Boundary Layer Separation," paper presented at AGARD Propulsion and Energetics

Panel 61st Specialists Meeting on Viscous Effects in Turbomachines, Copenhagen, Denmark, June 1983.

[2]Hobbs, D. E., Wagner, J. H., Dannenhoffer, J. F., and Dring, R. P., "Experimental Investigation of Compressor Cascade Wakes," ASME Paper 82-6T-299, 1982.

[3]Paterson, R. W. and Weingold, H. D., "Experimental Investigation of a Simulated Compressor Airfoil Trailing Edge Flowfield," Government Products Div., Pratt & Whitney Aircraft Group, West Palm Beach, Fla., Rept. FR-15859, Oct. 1982.

[4]Paterson, R. W. and Weingold, H. D., "Experimental Investigation of a Simulated Compressor Airfoil Trailing Edge Flowfield," AIAA Paper 84-0101, Jan. 1984.

[5]Paterson, R. W., Vogt, P. G., and Foley, W. M., "Design and Development of the United Aircraft Research Laboratories Acoustic Research Tunnel," *Journal of Aircraft*, Vol. 10, July 1973, pp. 427-433.

[6]Coles, D. E., "The Turbulent Boundary Layer in a Compressible Fluid," Rand Corp., Santa Monica, Calif., Rept. R-403-PR, Sept. 1962.

[7]Edwards, D. E., Carter, J. E., and Werle, M. J., "Analysis of the Boundary Layer Equations Including a New Composite Coordinate Transformation—The ABLE Code," United Technologies Research Center, East Hartford, Conn., Rept. UTRC81-30, May 1982.

[8]Haji-Haidari, A., "A Comparative Study of the Development of the Turbulent Near-Wake Behind a Thick Flate Plate with Both a Circular and Tapered Trailing Edge Geometry," M.S. Thesis, Lehigh University, Bethlehem, Pa., 1984.

[9]Roshko, A., "On the Drag and Shedding Frequency of Two-Dimensional Bluff Bodies," NACA TN 3169, July 1954.

[10]Owen, F. K., "Measurements of Unsteady Vortex Flow Fields," *AIAA Journal*, Vol. 18, Oct. 1980, pp. 1173-1179.

[11] Hinze, J. O., *Turbulence*, 2nd ed., McGraw-Hill Book Co., New York, 1979, pp. 496-507.